Preliminary Results on Join Wave Experiment Near Coast Around East China Sea during November and December, 2000

Beng-chun Lee, Chi-hao Chu, Lee-horng Leu and Chia-chuen Kao

ABSTRACT

The results of the wave models running operationally at Central Weather Bureau (CWB) for wave forecasts around East China Sea were compared against buoy observations, which one buoy from China and Taiwan respectively and two buoys from Korea, located near coast over East China Sea during November and December in 2000. This period was proposed by the WOM-4 meeting during September last year held in Taiwan. In this paper, there are two wave spectral models, include one is second-generation wave model and the other one is third generation of WAM model, to make wave analysis and forecast in this join wave experiment. The sea surface wind fields from Korea Meteorological Administration (KMA) model's products are as the initial input data to the wave models. Model outputs of wave heights taken from the grid point nearest to the buoy stations are the interesting data for the statistical error analysis. The error calculations are made by the mean bias error, the root mean square error, the correlation coefficient, and the scatter index for the forecast hours +00-, +24-, +48-hour.

1. INTRODUCTION

In order to improve the wave forecast technique so as to improve the safety of marine navigation as well as waterfront recreational activity and to mitigate coastal disasters, a series of workshops has been held by APEC/MRC/OMISAR in the past years. According to the conclusion of the WOM-4 (APEC, 2000), which was held on September 19-20, 2000 in Tainan, Chinese Taipei, one of the main goals of this workshop is to improve the wave forecasts by sharing the experiences in operational wave model forecasting among APEC member economies. Wave modelers, both for operational model and/or research model, are welcome to present their model results in the workshop.

One of the conclusions of the WOM-4 (APEC, 2000) suggested carrying out a joint experiment, in which the specialists run their on-hand wave forecast model(s) by using the same wind field data and the observed buoy wave data in order to form a common base for comparison and discussion. Specialists from all member economies are welcome to freely take part. A common data bank has been set up by OMISAR project, in which Korea Meteorological Administration (KMA) of Korea and the National Oceanic and Atmospheric Administration (NOAA) of United States contribute the wind field data for model input and State Oceanic Administration (SOA) of China, Central Weather Bureau (CWB) of Chinese Taipei and KMA of Korea offer the observed buoy wave data for model validation.

In this paper, the second-generation wave model (called CWB2G) and third generation of WAM model are used to make wave analysis and forecast in the join wave experiment. And model results of the wave hind casting and prediction are to be compared with the buoy data by using statistical errors to evaluate the model forecast skill.

2. FIELD EXPERIMENT AND DATA SET

According to the WOM-4 conclusion, each member economic may determine its own experiment domain. However, in order to make an intensive discussion possible, it is suggested that East China Sea be set as a preferable experimental domain. The experiment period is set to be November and December 2000, and a common data bank has been set up in Chinese Taipei accordingly.

The common data bank set up in the OMISAR project consists of the wind field data and the observed buoy data shown in Table 1 and 2. In which, the numerical grid wind fields are contributed by KMA and NOAA, and the buoys data are offered by KMA, SOA, and CWB respectively.

3. THE CWB BUOY NETWORK

In response to the need for more meteorological and oceanographic data around Taiwan waters, the CWB has been corporate with Coastal Ocean Monitoring Center (COMC) since 1994 to develop an operational data buoy observing systems. At present, there are a total of 3 stations in operations. The water depth of buoy stations is 31m, 32m, 23m for the Hualien, Lungtung, and Hsinchu, respectively. They are primarily located in near shore areas to provide real-time marine meteorology data.

The CWB operational data buoy system including: buoy hull, mooring, measurement instruments, data acquisition and control, data processing and analysis, communication, power, and auxiliary sub-systems has been successfully designed, integrated and deployed for marine meteorology observations.

Considering the operational requirements of low cost of manufacture and refurbishment, lightweight, land and sea transportability, wave-following characteristics, and reliability, the buoy was designed as a 2.5 meters discus-shaped foam buoy to be easily and safely handled without special equipment or procedures. The typical outlook of data buoy is also shown in Figure. 1.

Data measured and reported from the buoy include wind speeds, directions, and gusts; air and water temperatures; barometric pressures; and wave energy spectra from which significant wave heights, dominant and average wave periods, and directional wave information are derived. The corresponding payload capabilities are listed in Table 3. However, there are some more spare channels for future expansion on measuring other items such as tides, precipitation, humidity, and water quality, etc. The raw time-series data is stored on a data logger. Only some preprocessed data and parameters are then automatically transmitted to the ground receiving station every two-hour at assigned times by radio telemetry and immediately relayed to monitor center via telephone modem. Allowed for more frequent data acquisition of typhoon monitoring, the ground station could also be triggered to distribute the real time data on request.

Automated data quality control performed in real time is followed up in COMC. Following final data checks by experienced data analysts, data are processed, message formatted, and submitted to the CWB for use by operational forecasters in less than 30 minutes. The suspected or bad data identified will be kept in COMC for more advanced quality checks to prevent their distribution. The so-called "man-machine mix" QC procedures have been developing and refining at COMC for a few years to provide the highest quality data sets.

4. THE WAVE MODEL

4.1 CWB2G model

CWB2G model is the second-generation wave spectral model. The numerical techniques of this

model are based on the Golding(1983) and Chao(1993) proposed structures. According to Hasselmann (1962), the evolution of the spectrum can apply the energy balance equation to demonstrate as follows:

$$\frac{\partial E}{\partial t} + \vec{C}_g \cdot \nabla E = S \qquad (1)$$

Where E is the energy spectrum density function of the wave field, with frequency f, propagating direction θ, space coordinate x and time t; while $\vec{C}_g$ is the group velocity of the wave spectrum components f, θ, S is the source function of the wave energy generation. Symbol ∇ indicates two-dimensional calculations. If the seawater depth changes are taken into account, the group velocity and propagating direction will change as time elapses during the evolution process of the wave energy spectrum. Then Eq. (2) can be written as

$$\frac{\partial E}{\partial t} + \nabla \cdot \left(\vec{C}_g E\right) + \frac{\partial}{\partial \theta}\left[\left(\vec{C}_g \cdot \nabla \theta\right) E\right] = S_{in} + S_{ds} + S_{nl} \qquad (2)$$

Where S_{in} indicates the wave energy induced by the wind, S_{ds} is the wave energy induced by white capping and the effect due to sea bottom topography, S_{nl} is a new redistribution of wave energy induced among wave spectrums due to the nonlinear waves and the conservation among wave interactions.

There are four steps to resolve the equation: propagation, refraction, growth and decay, and nonlinear effects.

1.Propagation

On the aspect of wave propagation, forecast and revision are two processes to intercross grid system in order to minimize the decay and diffusion resulted from the numerical methods. Along the seashore area, the upstream difference scheme is exploited to insure that there is no wave refraction from the landmass.

2.Refraction

On the aspect of the refraction effect, the central difference scheme is used to calculate the water depth variations in the space. The refraction calculation method of the propagating direction is the same as the wave propagation scheme.

3. Growth and decay

On the aspect of wave growth, it is to apply the stimulating linear growth induced by the sea surface level turbulent disturbances and the exponential growth induced by the sea level already existing waves and average wind stress coupling effect. On the wave decaying side, only the white capping effects are considered. Along the shallow sea water areas, the energy loss caused by sea bottom frictions are added.

4.Nonlinear effect

On the aspect of the energy transformation of the nonlinear wave, the parameter of experience is applied. First, wave spectrum is concerned: the peak frequency is above 0.8; the intersection angle of the direction of wind and the wave propagation is within 90 degree. Also, it is suppose that the wind wave spectrum is through the nonlinear process, and it confirms to JONSWAP spectrum. Upon revising JONSWAP spectrum, any saturation of water depth and diffusion function should be taken into account.

4.2 WAM model

The CWB now applies the fourth revised edition of WAM model (Gunther et al., 1992). Within the

model, the basic equation is the wave energy propagation equation in relation to any specific spot on the sea surface with spectrum E (φ, λ, f, θ, t), where (φ, λ) are latitude and longitude of any specific spot on sea surface, it's a wave field of two dimensional frequency (f) and direction (θ).

$$\frac{\partial E}{\partial t}+\frac{\partial\left(C_{\varphi}E\right)}{\partial\varphi}+\frac{\partial\left(C_{\lambda}E\right)}{\partial\lambda}+\frac{\partial\left(C_{\theta}E\right)}{\partial\theta}=S_{in}+S_{ds}+S_{nl} \qquad (3)$$

Where (C_φ, C_λ, C_θ) are the phase speeds of wave energy propagation on (φ,λ,θ) coordinates, S_{in} is the wave energy influx transferred to waves from winds, S_{ds} is the depletion flux of wave energy, and S_{nl} is the energy propagation flux induced by the nonlinear effects caused by component waves.

(1) Wave energy influx, S_{in}

In the past, S_{in} is only assumed as a function of wind and has nothing to do with waves. This is incorrect, because it should be closely related to the wind speed and wave generation stress. Thus the growth rate of wave energy is related to friction velocity and roughness parameter.

(2) Depletion flux of the wave energy, S_{ds}

It is to consider the breaking waves and white capping will cause energy depletion. In the shallow water, being due to sea bottom friction to cause wave energy flux depletion should be added.

(3) The energy propagation flux due to nonlinear effects, S_{nl}

It is due to nonlinear effects that cause component waves will propagate wave energy flux among themselves. This phenomenon is based on oscillations of four component waves proposed by Hasselmann(1962). And the Boltzmann integration formula is derived to do calculations. But it is due to longer calculation time used, thus it is not suitable for operational forecast model, which the discrete intersection asymptotic method is applied in the third generation model to apply Boltzmann integration formula. This method applies only about 20% subset wave oscillation to do calculation. S_{nl} needs be revised. The revision is not compatible to the oscillation theory of the shallow water waves, but before securing the accurately effective shallow water theorem; it is just apply it for convenience.

5. EXPERIMENT RESULTS

A statistical error analysis (Lee, 2000) is performed for the model output of the significant wave height by using buoy measurements as the standard of reference. As for model, wave heights are taken from the grid point nearest to the buoy location. Since no single statistical indices are calculated for this study. The indices consist of the mean bias error *BIAS,* root mean square error *RMS,* correlation coefficient *CR* and scatter index *SI*. These indices take the forms

$$BIAS=\frac{1}{N}\sum\left(P_i-O_i\right) \qquad (4)$$

$$RMS=\left\{\frac{1}{N}\sum\left(P_i-O_i\right)^2\right\}^{1/2} \qquad (5)$$

$$CR=\frac{\sum\left[\left(P_i-\overline{P}\right)\left(O_i-\overline{O}\right)\right]}{\left\{\sum\left(P_i-\overline{P}\right)^2\sum\left(O_i-\overline{O}\right)^2\right\}^{1/2}} \qquad (6)$$

$$SI=RMS/\overline{O} \qquad (7)$$

Where N is the number of data points, and $\overline{P}$ and $\overline{O}$ are the means values of model predictions, P_i, and measurements, O_i, respectively

Buoys installed by KMA, SOA and CWB are all near coasts and about 30 meters deep below the sea level. The observed data from these buoys are different from those in the open sea. Besides, according to the completeness of the observed data to proceed the analysis (Table 4), buoy data of CWB are the most complete ones among the three, and data collected from buoys installed by KMA and SOA have less deficiency in December. Therefore, this paper chooses the collected data of December to investigate the research conditions on the aspect of statistical errors as analyzing model inductions and the in-situ observed values.

The statistical errors (Table 5 to Table 24) are computed to understand the performance of the model capability on wave height forecasts. Some preliminary results are address as follow.

At 00 hour forecast, within values of BIAS showing that results of model analysis, CWB model (CWB2G, WAM) has its induced values smaller than the observed ones near Lung-tung Buoy. And other three buoys have their induced ones larger than the observed ones in the results of model analysis. The correlation analysis (CR) also shows that the correlated values of model induced values and the observed values are rather high in KMA buoys. This indicates that there is a good correlation between the winds and waves. As for 12 hour forecast, results of BIAS show that CWN2G model forecast results and 00 hour analysis have the same characteristics with the results of model forecasts larger than the observed ones as forecast time spans increase, such 24 hour, 36 hour, etc. As for other error parameters, such as RMS indicates that the error values will increase with increasing forecasting time spans. CR also show the correlated values decrease as forecasting time spans increase.

During this join wave experiment, some weather patterns (Figure 2 to Figure 7) influence Taiwan area and make significant wave conditions there (Figure 8).

Pattern 1. Typhoon hit Taiwan accompanied with northeasterly monsoon circulations.

Typhoon Xangsane, from October 31 to November 1st, 2000, hit Taiwan area and made great damages over the island. During this invading period, the typhoon circulation associated with northeasterly monsoon strengthened the Taiwan local winds. The principal cause was just the strong pressure gradient force.

Pattern 2. Double influence between the typhoon circulation and the front system accompanied with the northeasterly monsoon.

Typhoon Bebinca, from November 3rd to 7 th, 2000, moved westward from east seawaters of Philippine to the South China Sea. Right at the very moment, there was a high-pressure system moving eastward from the Mainland China. Since the high-pressure system was not very strong and well organized, so the wind and wave status revealed the normal conditions at Lung-tung buoy station.

Pattern 3. Strong cold surges break over main China.

Strong cold surges out broke 2 times; November 10 to 14, December 11-12,2000 over main China. They moved southeastward and brought strong winds and cold temperatures down to the Taiwan area, thus making the meteorological unstable conditions very unstable around Taiwan area and over seawaters and causing sea surface temperature larger than that of the air temperature.

Pattern 4. Typical front systems.

In general, like the wintertime, such as November 15 – 18, November 20 – 22, and November 26 – 27, 2000, low-pressure system associated obvious frontal system will cause strong temperature contrasts along the frontal system. Besides, there is always a high-pressure system behind this obvious contrast (i.e. front). So, the obvious contrasts of meteorological factors (temperatures, wind directions, etc.) are the main causes.

Pattern 5. Northeasterly monsoon.

Northeasterly monsoon is the leading factor that causes the cold highs in the Mainland China to let out their strengths (temperatures are very low, winds are northeasterly and rather strong) to prevail around the Taiwan area and seawaters. Such as cases during November 23- 25, December 3-8, and December 23-31, 2000.

Pattern 6. Near stationary front system around Taiwan will cause unstable conditions over Taiwan seawaters and land areas, such as December 16 – 20, 2000.

6. DISCUSSIONS AND SUGGESTION

From the observed success rate of four buoy observation data in this experiment, obviously data from Lungtung Buoy is the best. It is mainly due to CWB'S trusting COMC to maintain the buoys. Besides, the periodic daily quality control is carried out on schedule, and conditions of the buoy operations are monitored by close attention. Once fallacy occurs, the maintenance work, under the permissible sea condition, is carried out immediately. Such cooperative mode of observation stations' management and maintenance between government operation units and research units can be served as example for other nations in the world to follow. And Chinese Taipei is very willing to provide such experience to share with others.

Taiwan is situated to the southeastern sea area of the Mainland China; there are no shielding to the north and the east of Taiwan. Therefore, from the point view of fetch during the winter, waves will come down to the vicinity of Taiwan from the north or the northeast with a consistent relationship between wave heights and weather types. Which, from the forecasting point of view, indicates that it is quite important to establish the relationship between the weather patterns and the local growth-decay conditions: then, according to the numerical wave results to revise forecast, thus the reliability can be improved.

From results of this experiment, it appears that the observed wave values and deduced values from the wave model or the forecasting tendency coincide with one another quite consistently. As CWB applies two models, WAM and CWB2G, to deduce and it is found out that, when applied around the Korean sea areas, the deduced values from the model are smaller than those from the observations with a specific case, a cold outbreak occurring on December 10th, whose deduced values were larger than those of the observed values. As applied around the Taiwan sea areas, the deduced values from the model are generally larger than those from the observed values. This requires further investigation and analysis.

The monitoring systems produce essential data for researchers in understanding the physical phenomenon and in developing and operating forecasting models. So the important mission is to develop and upgrade the large scale and coastal models. These can be a useful and effective approach to the prediction of marine and coastal environmental phenomena (including high water level, big wave, etc.). That is important to public safety and human well being, the national economy, and environmental management. Such data can also be useful in the decision-making process, in issuing warning messages, in studying coastal subsidence and erosions.

REFERENCE

APEC, 2000: Proceedings on The Fourth Workshop on Ocean Models for the APEC Region (WOM-4). September 19-20, 2000, Tainan, Chinese Taipei.

Chao, Y.Y., 1993: Implementation and evaluation of the Gulf of Alaska Regional Wave Model. NMC OPC Office Note 35pp.

Golding, B, 1983: A wave prediction system for real time sea state forecasting.

Quart. J. R. Met. Soc.109, 393-416.

Gunther, H., Hasslmann, S., and Janssen, P.A.E, 1992:Report NO.4, The WAM Model Cycle 4,Edited by Modellberatungsgruppe, Hamburg.

Hasselmann, K, 1962: On the nonlinear energy transfer in a gravity-wave spectrum.1.General theory, JFM, vol. 12, pp481-500.

Lee, B.C., 2000: Forecast results with CWB operational wave models during July 2000. Proceedings on The Fourth Workshop on Ocean Models for the APEC Region (WOM-4). pp1 .1-1.7.

Table 1 Wind field data (both forecast and analysis)

Contributor	KMA, Korea (Global)	KMA, Korea (Regional)	NOAA, USA
Domain	99E-160E, 0N-60N	115E-150E, 20N-50N	99E-150E, 0N-60N
Resolution	0.5 x 0.5	0.25 x 0.25	1 x 1
Data frequency	12UTC	00, 12UTC	00, 12UTC
Data length	Nov.1-Dec.31, 2000	Nov.1-Dec.31, 2000	Nov.1-Dec.31, 2000

Table 2 Observed Buoy data

Contributor	SOA, China	CWB, Chinese Taipei	KMA, Korea
Location	36.1N, 120.3E	25.01N, 121.91E	37.14N, 126.01E 34.48N, 125.46E (2 buoys)
Data type	Wind Speed and Direction Wave height, Hs Wave Period, Ts	Wind Speed and Direction (2 sensors) Wave Height, Hs Wave Period, Ts	Wind Speed and Direction (2 sensors) Wave Height, Hs Wave Period, Ts
Data frequency	2 hours	2 hours	1 hour
Data length	Dec 11-31, 2000	Nov 1-Dec 31, 2000	Nov 1-Dec 31, 2000

Table 3 Data buoy payload capabilities

Parameters	Range	Resolution	Accuracy
Wind speed	0-60 m/sec	0.1 m/sec	1 m/sec
Wind direction	0-360 °	1.0 °	10 °
Air temperature	0-50℃	0.1 ℃	1 ℃
Water temperature	0-50℃	0.1℃	1 ℃
Barometric pressure	900-1100mb	0.1mb	1mb
Significant wave height	0-20 m	0.1 m	0.2 m
Wave period	3-30 s	0.1 s	1 s
Wave spectra	0.03-0.40Hz	0.01 Hz	

Table 4 wave record in buoy stations

Month	KMA-22101	KMA-22102	SOA	CWB
11	232/720	233/720	-	356/360
12	670/744	687/744	158	318/372

Table 5 Statistical errors between forecast wave height +00-hr
for buoy-KMA 22101 during December 2000

Model	BIAS	RMS	CR	SI
WAM	-0.165	0.342	0.818	0.457
CWB2G	-0.330	0.477	0.761	0.64

Table 6 Statistical errors between forecast wave height +00-hr
for buoy-KMA 22102 during December 2000

Model	BIAS	RMS	CR	SI
WAM	-0.217	0.453	0.851	0.369
CWB2G	-0.346	0.571	0.886	0.322

Table 7 Statistical errors between forecast wave height +00-hr
for buoy-SOA during December 2000

Model	BIAS	RMS	CR	SI
WAM	-0.131	0.375	-0.102	0.579
CWB2G	-0.347	0.485	-0.331	0.749

Table 8 Statistical errors between forecast wave height +00-hr
for buoy-CWB during December 2000

Model	BIAS	RMS	CR	SI
WAM	0.083	0.599	0.570	0.387
CWB2G	0.249	0.960	0.574	0.621

Table 9 Statistical errors between forecast wave height +12-hr
for buoy-KMA 22101 during December 2000

Model	BIAS	RMS	CR	SI
WAM	0.201	0.441	0.794	0.588
CWB2G	-0.009	0.258	0.863	0.344

Table 10 Statistical errors between forecast wave height +12-hr
for buoy-KMA 22102 during December 2000

Model	BIAS	RMS	CR	SI
WAM	0.083	0.808	0.621	0.657
CWB2G	-0.034	0.396	0.886	0.322

Table 11 Statistical errors between forecast wave height +12-hr
for buoy-SOA during December 2000

Model	BIAS	RMS	CR	SI
WAM	0.156	0.530	-0.012	0.817
CWB2G	-0.047	0.445	-0.215	0.687

Table 12 Statistical errors between forecast wave height +12-hr
for buoy-CWB during December 2000

Model	BIAS	RMS	CR	SI
WAM	0.096	0.584	0.607	0.378
CWB2G	0.508	1.104	0.563	0.714

Table 13 Statistical errors between forecast wave height +24-hr for buoy-KMA 22101 during December 2000

Model	BIAS	RMS	CR	SI
WAM	0.438	0.697	0.696	0.930
CWB2G	0.083	0.334	0.774	0.446

Table 14 Statistical errors between forecast wave height +24-hr for buoy-KMA 22102 during December 2000

Model	BIAS	RMS	CR	SI
WAM	0.215	0.737	0.697	0.599
CWB2G	0.132	0.518	0.818	0.421

Table 15 Statistical errors between forecast wave height +24-hr for buoy-SOA during December 2000

Model	BIAS	RMS	CR	SI
WAM	0.397	0.702	0.085	1.083
CWB2G	0.112	0.478	-0.087	0.737

Table 16 Statistical errors between forecast wave height +24-hr for buoy-CWB during December 2000

Model	BIAS	RMS	CR	SI
WAM	-0.008	0.502	0.527	0.325
CWB2G	0.215	0.654	0.649	0.423

Table 17 Statistical errors between forecast wave height +36-hr
for buoy-KMA 22101 during December 2000

Model	BIAS	RMS	CR	SI
WAM	0.616	0.827	0.730	1.103
CWB2G	0.174	0.420	0.671	0.561

Table 18 Statistical errors between forecast wave height +36-hr
for buoy-KMA 22102 during December 2000

Model	BIAS	RMS	CR	SI
WAM	0.569	1.045	0.650	0.850
CWB2G	0.395	0.753	0.737	0.613

Table19 Statistical errors between forecast wave height +36-hr
for buoy-SOA during December 2000

Model	BIAS	RMS	CR	SI
WAM	0.581	0.899	0.110	1.388
CWB2G	0.202	0.508	0.002	0.784

Table 20 Statistical errors between forecast wave height +36-hr
for buoy-CWB during December 2000

Model	BIAS	RMS	CR	SI
WAM	0.089	0.561	0.436	0.363
CWB2G	0.234	0.707	0.496	0.457

Table 21 Statistical errors between forecast wave height +48-hr
for buoy-KMA 22101 during December 2000

Model	BIAS	RMS	CR	SI
WAM	0.873	1.085	0.649	1.499
CWB2G	0.248	0.480	0.602	0.641

Table22 Statistical errors between forecast wave height +48-hr
for buoy-KMA 22102 during December 2000

Model	BIAS	RMS	CR	SI
WAM	0.820	1.263	0.622	1.027
CWB2G	0.607	0.922	0.681	0.750

Table 23 Statistical errors between forecast wave height +48-hr
for buoy-SOA during December 2000

Model	BIAS	RMS	CR	SI
WAM	0.760	0.932	0.181	1.438
CWB2G	0.275	0.515	0.043	0.794

Table 24 Statistical errors between forecast wave height +48-hr
for buoy-CWB during December 2000

Model	BIAS	RMS	CR	SI
WAM	0.223	0.762	0.267	0.493
CWB2G	0.354	1.049	0.242	0.679

Figure 1 CWB'S Buoy

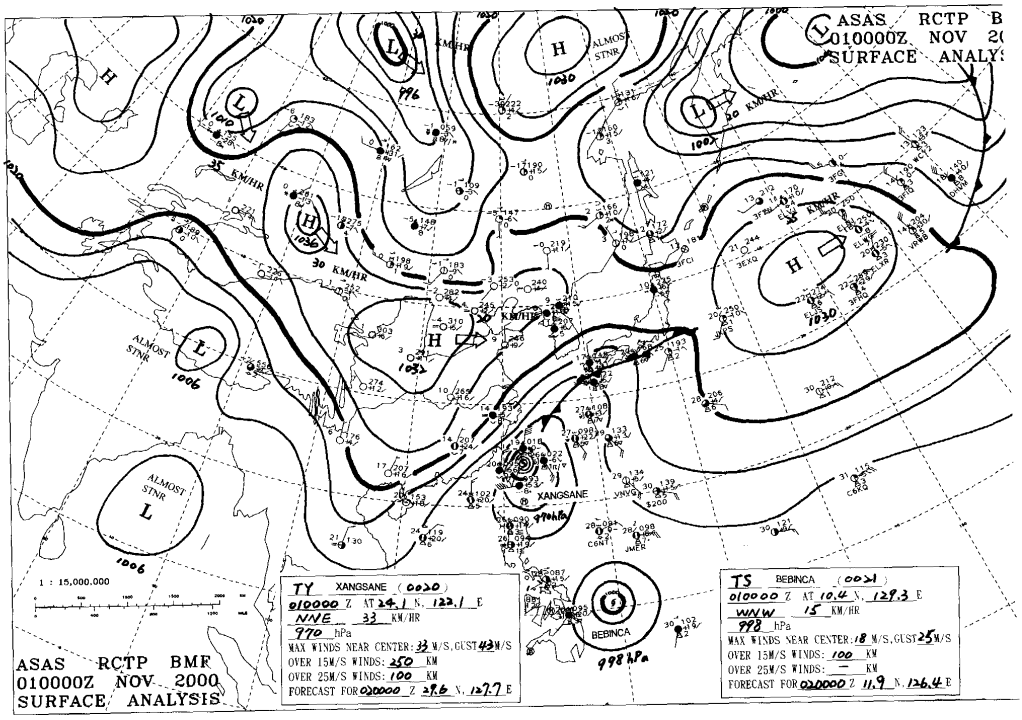

Figure 2 Typhoon hit Taiwan accompanied with northeasterly monsoon circulations.

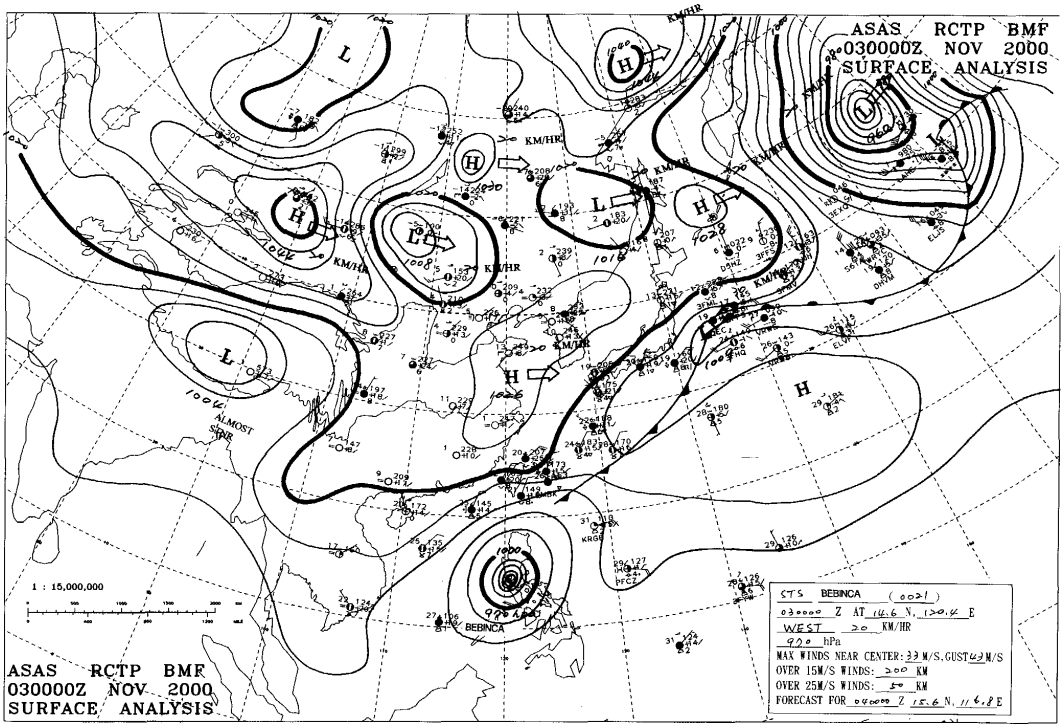

Figure 3 Double influence between the typhoon circulation and the front system accompanied with the northeasterly monsoon.

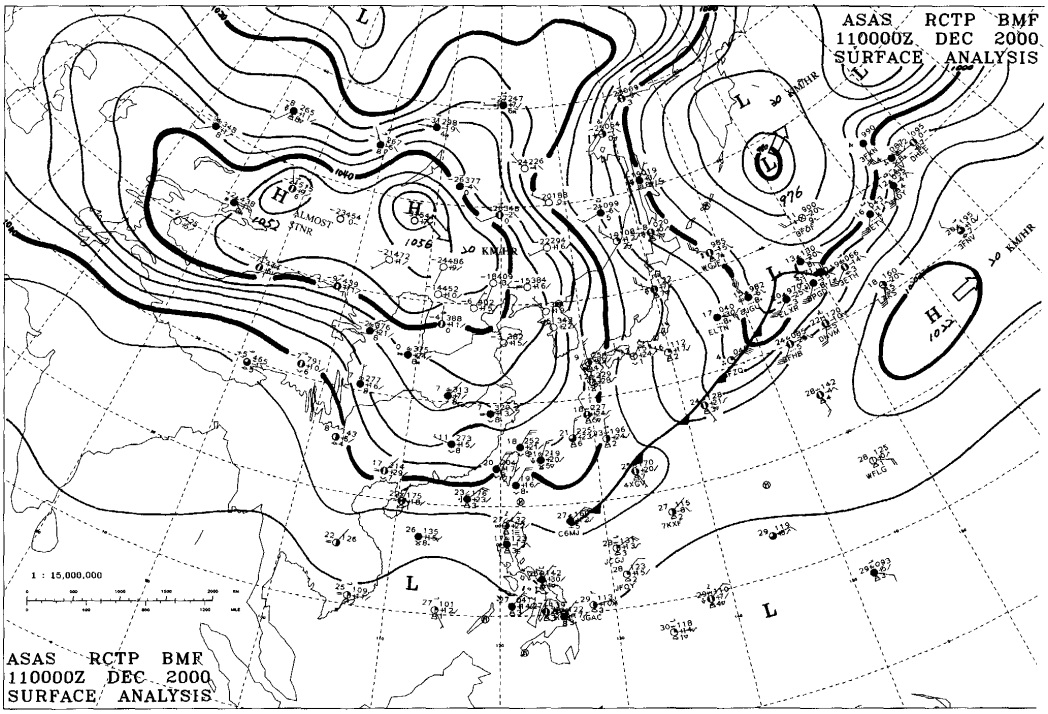

Figure 4 Strong cold surges break over main China.

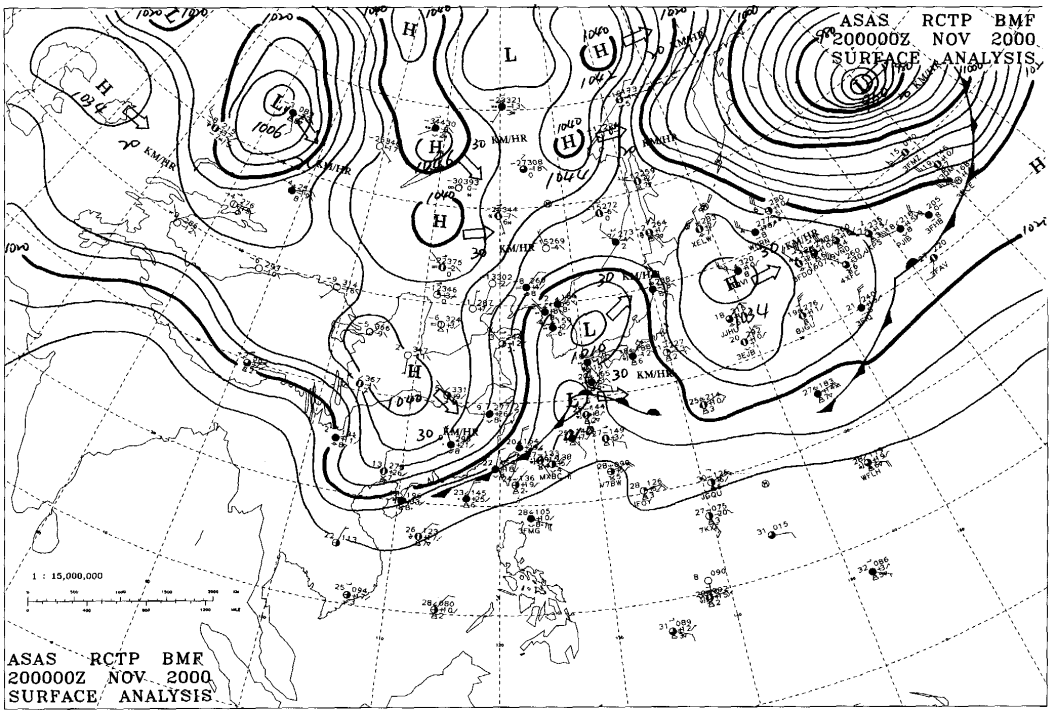

Figure 5 Typical front systems.

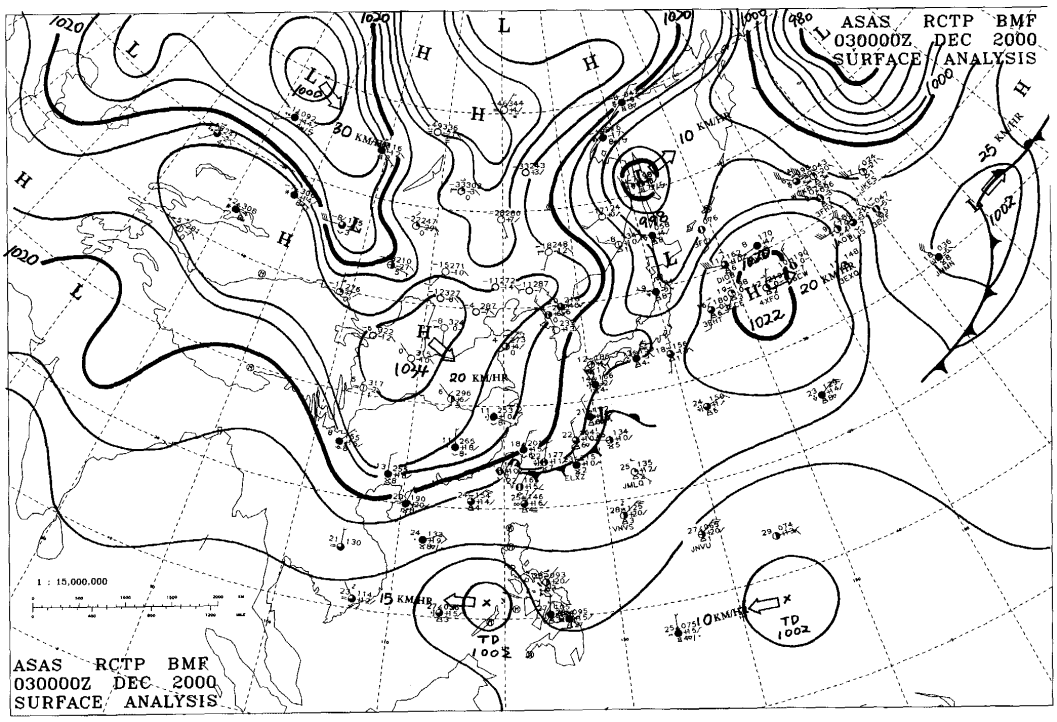

Figure 6 Northeasterly monsoons.

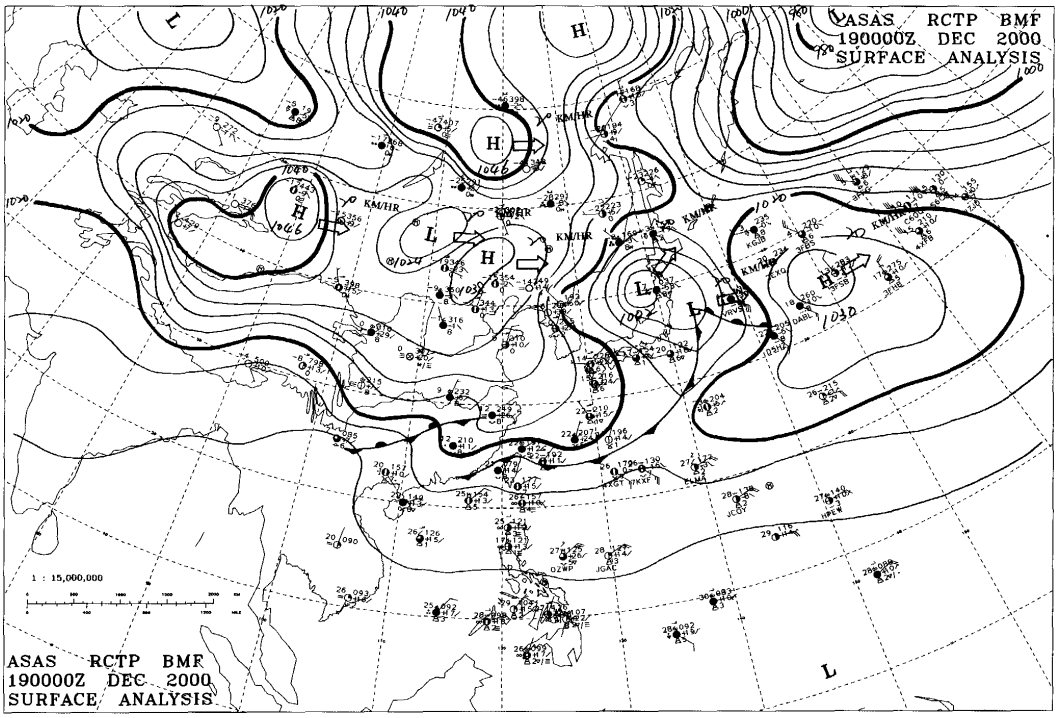

Figure 7 Near stationary front systems around Taiwan.

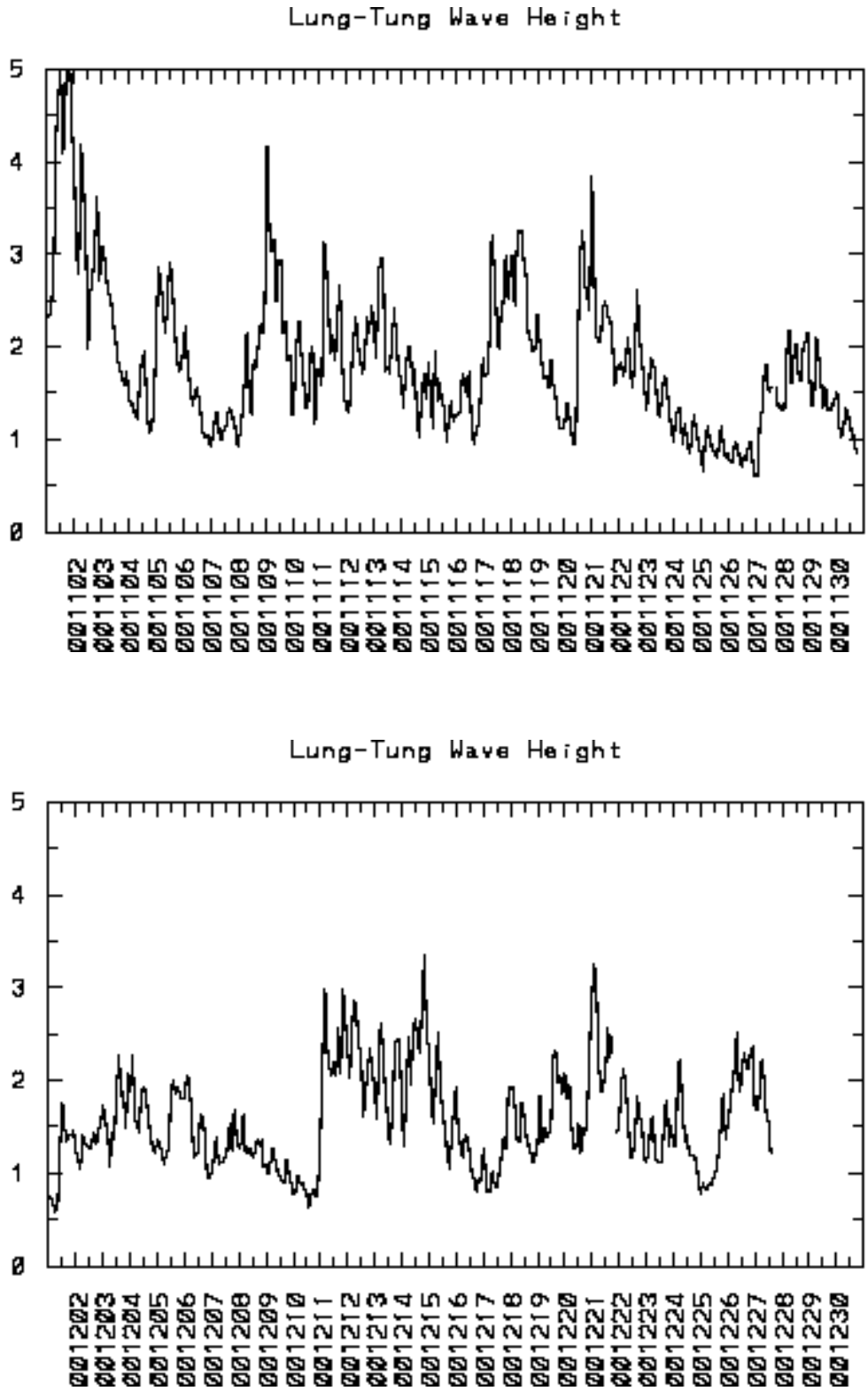

Figure 8 Wave records in Lung-tung Buoy station